

FEASIBILITY STUDY OF USING THERMAL SIMULATOR TO OBSERVE METALLURGICAL ASPECTS OF WELDING DUPLEX STAINLESS STEEL

¹FUAD KHOSHNAW, ²VERONIQUE VITRY, ³FABIENNE DELAUNOIS

¹Senior Lecturer, School of Engineering and Sustainable Development, De Montfort University –United Kingdom

²Associate Professor, Metallurgy Department, Polytechnique Faculty, University of Mons – Belgium Veronique.

³Professor, Metallurgy Department, Polytechnique Faculty, University of Mons – Belgium Fabienne.

E-mail- ¹Fuad.hassankhoshnaw@dmu.ac.uk, ²VITRY@umons.ac.be, ³DELAUNOIS@umons.ac.be

Abstract - This study focused on using thermal cycle simulator to investigate the metallurgical modifications that occur during welding of austenitic stainless steel type 304L and duplex stainless steel alloy type 2205. Thermal cycle simulator is known as an effective method to simulate the HAZ in the welded samples. Hence, the temperatures that are applied through this method should not reach the melting temperatures of the welded material. Different peak temperatures, from 500 to 1100°C were applied on the samples. Although the whole heating and cooling process was relatively short and did not exceed 7 minutes, both alloys were subject to metallurgical changes such as carbide precipitation in austenitic alloy and ferrite : austenite ratio in duplex alloy. The amount of carbide precipitation increased for longer exposure at specific temperatures. The amount of ferrite contained in duplex alloys increased with increasing peak temperature. However, other phases did not appear noticeably within this period, 7 minutes, at the peak temperatures applied in this study.

Keywords - Thermal Cycle Simulation, Chromium Carbide Precipitation, Austenitic Stainless Steel, Duplex Stainless Steel, Ferrite Content.

I. INTRODUCTION

Day after day the demand for stainless steel alloys is noticeably increasing [1]. This demand has become higher than ever before for duplex alloys, and this can be attributed to their microstructure comprised of both ferrite and austenite, which provides better properties than the two phases taken separately [2, 3]. In general, both austenitic and duplex alloys provide good mechanical properties, high corrosion resistance and sufficient level of weldability. As a result, they have become one of the most preferable alloys for the applications which require these properties [4, 5].

However, welding remains one of the major challenges that stainless steel alloys are facing because of the microstructural changes that occur in the melted and heat affected zones (HAZ) [6, 2, 1, 7]. For example, austenitic stainless steel alloys is exposed to weld decay and intergranular corrosion due to chromium carbide precipitation. Khoshnaw [4] found that the carbide precipitation occurs when the alloy passes through the sensitization temperature ranges, i.e. 500 and 850°C. Subsequently this precipitation affects ductility, toughness and corrosion resistance. Similarly, duplex stainless steel alloys are exposed to embrittlement, in addition to carbide precipitation. Pardal [7] and Nuria Llorca-Isen [8] showed that some brittle phases such as Chi and Sigma phases form in temperature ranges between 600 and 1000°C at different periods of time. On the other hand, heating affects the austenite: ferrite ratio in duplex steels, as a result this will affect the mechanical and corrosion properties. Therefore, research is continuously ongoing to keep the negative impacts of welding processes on the mechanical

properties and corrosion resistance of stainless steel alloys as limited as possible.

In the last few decades, numerous studies have been carried out to investigate the negative impacts of welding on the mechanical properties and corrosion resistance of stainless steel alloys. The modifications are always referred to the metallurgical aspects that occur in the fusion zone and HAZ. However, because these two zones are relatively narrow and present intermixing, especially in the arc-based welding processes, e.g. TIG and MIG, finding an accurate contribution of each zone towards the type and amount of microstructural changes, has become a focal point of discussion. Thus, to overcome this confusion, different thermal simulation methods [9, 10, 11, 12, 6] have been used as an experimental method to provide relatively quick information that reflects the thermal configuration of different welding processes.

To investigate the metallurgical modifications that happen during welding, researchers have started thermal simulation by heating samples using conditions that reproduce as best as possible the welding process, especially for HAZ. Thermal cycle simulation of HAZ is achievable through the use of thermal simulator devices that heat the samples up to just below the melting point, as the equipment is not able to record the temperatures after the material has melted. Samardzic et al [9] used Smitweld type TCS 1405 weld thermal simulator and has found that it is a suitable device for accelerated investigation of weldability and presents relationship between cooling time at weld thermal simulating parameters and mechanical properties of weld joint in heat affected zone (HAZ). Kulhanek et al [13] worked on steel P92

and tried to compare the microstructures with hardness parameters, as they found identical and proved accuracy of temperature simulation. Mohyla et al[11] compared the mechanical properties and microstructure of HAZ of P92 welded joints made by TIG method and samples with simulated temperatures. The results showed relatively good agreement, as they found that using the thermal simulator brings reasonable, repeatable result and seems to be promising method how to investigate properties and microstructure of the HAZ. Scott et al[12] used thermal cycle simulations on a round robin test for high strength low alloys steel alloys to build a continuous cooling transformation diagram. They showed that despite the small number of laboratories involved and scattered results, it was still possible to show that this approach gives reasonable results, but with a certain degree of inaccuracy.

Understanding the metallurgical aspects that are associated with the welding processes requires careful investigation. Thermal simulation techniques can help to characterise the subsequent changes of the microstructure at specific temperatures which have similar heating and cooling rates to the welding process. This method has been applied on the materials which are frequently used in applications that require welding such as steel, aluminium, titanium and stainless steel alloys. Since there are only limited number of researches studied this technique on duplex stainless steel alloys, this study aims to investigate the feasibility of using thermal simulation on duplex stainless steel alloy type 2205 and austenitic stainless steel type 304L as a control alloy.

II. EXPERIMENTAL WORKS

The thermal cycle simulator type SMITWELD [9, 13, 12], is used to simulate the thermal cycles at different peak temperatures for each alloy. The process is aimed to provide quick simulation of temperature cycles, which reflect similar circumstances to those that occur during welding, while providing an enlarged HAZ due to geometry of the equipment and samples. This equipment provides thermal cycling by applying high current and low voltages through two probes positioned at the extremities of a metallic sample, which lead to heat up the centre of sample to the selected temperature. Due to the presence of water-cooling systems on the extremities of the samples, a temperature gradient similar to that of HAZ is formed in the samples and, after heating it is cooled down to room temperature.

Austenitic type AISI 304L and duplex stainless steel alloy type 2205 (UNS S32205) have been used in this study. Their chemical analysis is shown in Table 1. Square cross section samples with a section of 10x10 mm, and a length of 70 mm were used in this study as

required by the geometry of the thermal cycle simulator.

| Alloy | Chemical Composition wt.% | | | | | | | |
|-------|---------------------------|------|-----|-----|-----|-----|-----|--------|
| | C | Cr | Ni | Mo | Mn | Si | Co | Rem |
| 304L | 0.03 | 18.1 | 8.2 | 0.4 | 1.9 | 0.3 | 0.2 | 0.1 V |
| 2205 | 0.03 | 22.9 | 4.1 | 6.8 | 1.4 | 0.8 | 0.4 | 0.13 N |

Table 1 chemical analysis of the alloys used in this study.

The temperature cycle applied to the samples was controlled through a computer programming that is installed with the thermal simulator, and the actual temperatures were measured by thermocouples attached to the samples by spot welding and thus recorded against time during the whole heating and cooling process. Figure 1 presents the heating system, with a sample installed for simulation and a single thermocouple for peak temperature measurement.

The thermocouples were attached in the middle of the samples, i.e. 35 mm from the extremities. However, several tests have been carried out with the use of multiple thermocouples on other locations on the sample (e.g. 10 mm from the middle) in order to determine the temperature distribution across the length of the sample and for calibration purposes. The recorded data (time/temperature evolution) was transferred into a spreadsheet file to be set up as a graph presenting heating and cooling rates for the various applied temperatures, to be used for subsequent interpretation of the microstructures.



Figure 1 Thermal cycle simulator type SMITWELD used in this study, complete with sample and single thermocouple.

Different peak temperatures were applied on each alloy. For austenitic alloys the range of peak temperature was 500 to 900°C, while it was 500 to 1100°C for duplex. These temperatures were selected on the basis of the range of sensitivity to chromium carbide precipitations and formation of brittle phases of austenitic and duplex alloys. Generally, the recorded temperatures were different from the intended temperatures; for example, for setting the device at 700°C the recorded temperature on the sample was showing 686°C in one run and 692°C in

the next run. This difference can be attributed to the thermal conductivity of the material itself and to the size of the spot-welded contact between the thermocouple and the sample.

On the other hand, to investigate the effect of time on the metallurgical phenomena in the used alloys, samples were isothermally heat treated in an electric furnace (type Carbolite CWF13/13) at 700°C for austenitic stainless steel and 750°C for duplex alloy for 3 different times: 5 min, 30 min and 60 min. The reason behind using this temperature for the isothermal treatments is because the results show that this range of temperature causes the highest sensitization in austenitic alloy. Hence, even higher temperature, i.e. 750°C was used on duplex alloy for comparison.

Ferrite measuring apparatus, type Ferritegehaltmesser, is used to determine the ferrite content after thermal cycle for the duplex alloys, that was then compared to the as-received samples [14]. The device determines the ferrite number, FN, based upon an arbitrarily defined relationship between the magnetic susceptibility of the samples and the ferrite content. The FN is converted to ferrite content (volume) percentage based on the following equation, as recommended by the device supplier:

$$\text{Ferrite Content \%} = 7.30583 \times e^{\frac{\text{FN}}{8.88399}} - 7.162$$

Macro-hardness HVT30 type Emco test automatic is used to measure the hardness of the samples.

Scanning electron microscope type JEOL-SEM 6400 is used to observe the microstructural changes. Two etching techniques were used in this study: (i) Electrochemical etching in oxalic acid for 60-90 seconds at room temperature applying 3 V, using device type Struers LecroPol-5, (ii) immersion in Murakami etchant for 2-3 minutes [15]. All the images in this study were taken at the etched conditions.

III. RESULTS AND DISCUSSION

Figures 2 and 3 show some of the thermal cycle simulation curves for austenitic and duplex alloys respectively. Not all the thermal cycle simulations are plotted in these figures to make clearer distinctions between the curves.

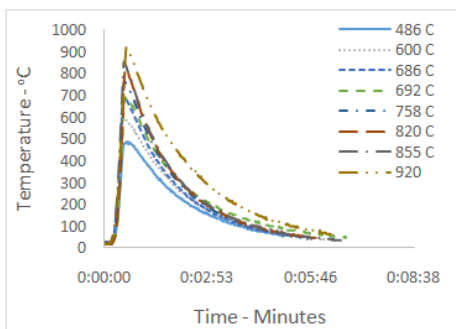


Figure 2 Thermal simulation curves for various applied temperatures on austenitic stainless steel alloy type 304L.

Table 2 shows the hardness values measured at the centre of the samples (middle) which is exposed to the highest temperature as well as the value obtained 10 mm from the central point (sides). The values are the average of 3 measurements on the same sample. The table shows also the hardness of as-received samples and of samples that were isothermally heat treated.

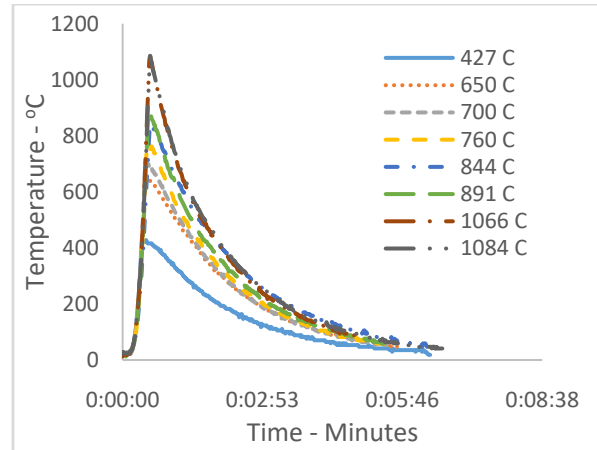


Figure 3 Thermal simulation curves for various applied temperatures on duplex stainless steel alloy type 2205.

Table 3 shows the effect of temperature on the ferrite content of duplex samples, in the centre (middle location) and side (10 mm from centre) location, for heat treated and heat cycled samples. Similar tests were applied to austenitic samples but the variations of the ferrite content were too small to be interpreted: less than 1% ferrite.

| Austenitic stainless steel | HVT30 | | Duplex stainless steel | HVT30 | |
|----------------------------|--------|-------|------------------------|--------|-------|
| | Middle | Sides | | Middle | Sides |
| As Received | 302 | 300 | As Received | 292 | 292 |
| 486°C | 292 | 290 | 427°C | 270 | 290 |
| 600°C | 287 | 287 | 650°C | 273 | 258 |
| 692°C | 294 | 306 | 760°C | 257 | 255 |
| 758°C | 288 | 280 | 844°C | 244 | 245 |
| 855°C | 230 | 230 | 920°C | 233 | 234 |
| 920°C | 180 | 180 | 1084°C | 250 | 258 |
| 700°C – 5 min | 245 | 243 | 750°C – 5 min | 258 | 255 |
| 700°C – 30 min | 244 | 245 | 750°C – 30 min | 269 | 273 |
| 700°C – 60 min | 250 | 228 | 750°C – 60 min | 268 | 272 |

Table 2 The hardness values of as-received and heated samples.

The applied temperatures in this study had been decided based on the range of sensitive temperatures for both alloys, which start at 500°C and then increasing by 100°C for each following sample up to 1100°C [2, 1, 4].

The temperatures that are considered in this study, as shown in Figures 4 and 5, reflect the actual temperatures at which samples have been heated. In

addition, the results of this study can be employed for the study of HAZ of similar alloy weldments, only when the welding process has the same heating and cooling rates similar to those used in this study. Figures 4 and 5 show the main metallurgical phenomena which occurred in austenitic and duplex stainless steel alloys respectively. These changes can be interrelated with the hardness values, Table 2, and the ferrite content %, Table 3.

| Duplex | Ferrite Content % | |
|----------------|-------------------|------------|
| | Middle | 10 mm Side |
| As Received | 40.2 | 40.2 |
| 427°C | 43.1 | 45.3 |
| 650°C | 42.7 | 42.8 |
| 760°C | 47.2 | 47.6 |
| 844°C | 47.3 | 49.8 |
| 920°C | 47.5 | 47.3 |
| 1084°C | 49.0 | 48.1 |
| 750°C – 5 min | 37.4 | 37.2 |
| 750°C – 30 min | 28.4 | 28.3 |
| 750°C – 60 min | 28.3 | 28.5 |

Table 3 Ferrite content % in duplex samples.

3.1 Austenitic Stainless Steel Alloy Type 304L

Figure 4 shows the microstructural changes of austenitic alloy type 304L. Fig. 4a shows the microstructure in as-received condition, with a small amount of retained ferrite. Figures 4b, c and d show the changes that happen due to heating the samples up to 486°C, 692°C and 920°C respectively. The figures show that the amount of chromium carbide precipitation at 486°C is higher than in the as-received sample, and that it increased noticeably at 692°C. The microstructural investigations showed that for temperatures higher than 692°C, the amount of carbides decreases with increasing temperature. Subsequently, the amount of carbides present after cycling at 925°C is almost the same as its for 486°C. This coincides with other researchers' results [4, 6] which show that the sensitization range of austenitic stainless steel sits within the 500-850 °C range. Above that temperature, the carbides start to dissolve in the solid solution.

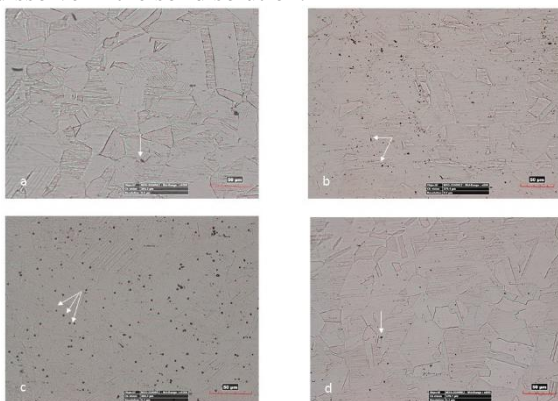


Figure 4 Microstructure of austenitic alloy: a: as-received, b: after heating at 500°C, c: after heating at 692°C, d: after heating at 920°C.

Table 2 shows that the hardness of the austenitic sample cycled at 500°C is lower than that of as-received austenitic sample, however hardness increases with temperature from 692°C, then decreases to a minimum at 920°C. This can be attributed to the precipitation of carbides, which are a hard phase. However at higher temperatures, these carbides dissolve, thus exposing the material to annealing and softening leading to a reduction of hardness.

Note: To show the growth of the precipitates consistently, all the indicated scale-bars on the microstructural photos in this study are 50 micron.

Figure 2 showed that the total time – heating and cooling - for each thermal cycle simulation did not exceed 7 minutes, while the heating to the peak temperature and cooling up to the lowest sensitization range of temperatures, 550°C is almost 1 minute, which is relatively short time to allow complete carbide precipitation, considering that this phenomenon occurs in the sensitized area during the actual welding process.

Accordingly, to observe the effect of exposure time on carbide precipitation at the temperature that give the highest sensitization, samples were isothermally heat treated at temperatures close to 692°C where the highest amount of carbide precipitation appeared - for 5, 30 and 60 minutes. Figure 5 shows that the carbides become thicker and denser on the grain boundaries with increasing heat treatment time. This confirms that 700°C sits in the range for which quick precipitation of chromium carbides occur in 304L stainless steel [13, 12, 9].

The hardness of sample heat treated at 700°C is similar for the three different treatment times but it is lower than that of the as-received sample and of the thermal cycled sample, due, for the latest, to a more important effect of matrix softening than of hard phase precipitation, and also to the excessive growth of carbides.

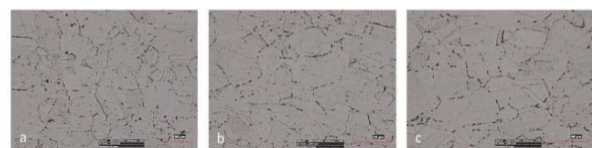


Figure 5 Effect of time on carbide precipitation in austenitic alloy at 700°C: a: 5 min, b: 30 min and c: 60 min.

3.2 Duplex Stainless Steel Alloys Type 2205

Figure 6 shows the microstructural changes in duplex 2205 alloy type. Metallographical observation showed that temperatures at 427, 650 and 760°C did not modify the microstructure significantly compared with as-received samples. Duplex alloys present effectively higher stability to microstructural changes than austenitic alloys, although low amounts of precipitation can be seen at 650°C and 760°C [5, 7, 1]. However, noticeable changes in microstructure started from 844°C and this has become noticeably

clear at 920°C and 1084°C. Figure 6d, 6e and 6f show noticeable changes started around 800°C following grain growth process at higher temperatures, producing longitudinal grains with uniaxial directions. This is in concordance with the hardness of the samples, as Table 2 showed, increasing the temperature decreased hardness, especially at 920°C, where the microstructure showed a complete recrystallization, i.e. the number of dislocations decreased.

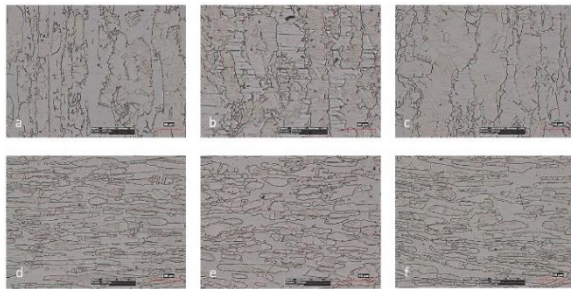


Figure 6 Microstructural changes of duplex alloy, a: as-received, b: after heating at 427°C, c: 650°C, d: 760°C, e: 844°C and f: 1084°C.

As mentioned in the previous paragraph, no microstructural changes were observed at 427, 650 and 760°C, however to examine the effect of time on carbide precipitation, samples were heat treated at 750°C for 5, 30 and 60 minutes. This is even higher than 700°C temperature which the 304L stainless steel samples were heated for similar period and showed changes in carbide precipitation. Figure 7 shows that – similar to austenitic alloy – the amount of precipitated carbides increases with time and precipitation is thicker and denser on the grain boundaries. This is evidence that 750°C is in the sensitization range for duplex alloys.



Figure 7 Carbide precipitation in duplex alloy at 700°C with time, a: 5 min, b: 30 min and c: 60 min.

The hardness evolution of duplex samples can be interpreted similarly to that of austenitic stainless steel: on one hand, carbide precipitation increases the hardness, on the other hand, cycling at high temperature causes softening and reduces the hardness. Therefore, the final result shows the balance between these two phenomena.

Table 3 shows that the amount of ferrite increases with raising temperature. The as-received sample contained 40% ferrite and this amount was raised to close to 50% at 1088°C. This result is similar to published literature that confirms increasing ferrite content with temperature [14, 4, 2]. However, the ferrite content of the isothermally treated samples was lower than that of the as-received sample. This can be

attributed to the amount of carbide precipitation: chromium being a ferrite stabilizing element, its precipitation at the grain boundaries as chromium carbide will lower the amount of ferrite.

IV. CONCLUSION

1. The thermal simulation is not sufficient to show the whole microstructure modifications in duplex alloy because of the short time remaining at sensitization ranges due to high heating and cooling rate.
2. The maximum amount of precipitation occurred at 700°C within around 1-2 minutes.
3. The amount of metallurgical changes increased with increasing time for the isothermally heat treated samples in both alloys.
4. The ferrite content increased with increasing cycling temperature.
5. Cycling at higher temperatures had dual effects on hardness. Hardness increased due to carbide precipitation and decreased due to softening.

ACKNOWLEDGMENTS

The authors acknowledge FNRS for funding (IN travel grant) for Fuad Khoshnaw, under the supervision of Professor Véronique Vitry. Thanks to head of the department Professor Fabienne Delaunoy for her administration support relevant to this work, PhD students Luiza Bonin, Alexandre Mégret and Victor Stanciu for their friendly support, also to the technicians Daniel Pouille and Sébastien Colmant, for their continuous support with experimental work.

REFERENCE

- [1] R. V. T. Jagesvar Verma, "Effect of welding processes and conditions on the microstructure, mechanical properties and corrosion resistance of duplex stainless steel weldments—A review," *Journal of Manufacturing Processes*, vol. 25, pp. 134-152, 2017.
- [2] B. Deng, Z. Wang, Y. Jiang, T. Sun, J. X. and J. Li, "Effect of thermal cycles on the corrosion and mechanical properties of UNS S31803 duplex stainless steel," *Corrosion Science*, vol. 51, p. 2969–2975, 2009.
- [3] Z. Zhang, H. Jing, L. Xu, Y. Han, L. Z. and J. Zhang, "Influence of microstructure and elemental partitioning on pitting corrosion resistance of duplex stainless steel welding joints," *Applied Surface Science*, vol. 394, pp. 297-314, 2017.
- [4] F. Khoshnaw and R. Gardi, "Sensitization assessment of duplex stainless steel using critical pitting temperature CPT method - ASTM G48," *Buletinul Institutului Politehnic Din Iasi*, vol. 3, pp. 261-268, 2007.
- [5] J. P. Pauline Boillot, "Use of stainless steels in the industry: recent and future developments," *Procedia Engineering*, vol. 83, pp. 309-321, 2014.
- [6] H. Tan, Z. Wang, Y. Jiang, Y. Yang, B. Deng, H. Song and J. Li, "Influence of welding thermal cycles on microstructure and pitting corrosion resistance of 2304 duplex stainless steels," *Corrosion Science*, vol. 55, pp. 368-377, 2012.
- [7] J. M. Pardal, S. S. M. Tavares, M. d. P. C. Fonseca, J. A. d. Souza, L. M. Vieira and H. F. G. d. Abreu, "Deleterious Phases Precipitation on Superduplex Stainless Steel UNS

- S32750: Characterization by Light Optical and Scanning Electron Microscopy," *Materials Research* , vol. 13, no. 3, pp. 401-407, 2010.
- [8] NúriaLlorca-Isern, HéctorLópez-Luque, IsabelLópez-Jiménez and M. VictoriaBiezma, "Identification of sigma and chi phases in duplex stainless steels," *Materials Characterization*, vol. 112, pp. 20-29, 2016.
- [9] Samardžić, A. Stoić, D. Kozak, I. Kladaric and M. Dunder, "Application of Weld Thermal Cycle Simulator in Manufacturing," *Journal of Manufacturing and Industrial Engineering* , pp. 7-11, 2013.
- [10] Z. Boumerzoug, E. Raouache and F. Delaunois, "Thermal cycle simulation of welding process in low carbon steel," *Materials Science and Engineering A*, vol. 530, p. 191–195, 2011.
- [11] H. J. H. L. K. Petr Mohyla, "Investigation of heat affected zone of steel P92 using the thermal cycle simulator," *International Journal of Materials and Metallurgical Engineering*, vol. 11, no. 6, pp. 460-463, 2017.
- [12] Scotti, H. Li and R. M. Miranda, "A Round-Robin Test with Thermal Simulation of the Welding HAZ to draw CCT diagrams: a need for harmonized," *Journal Soldagem & Inspeção*, vol. 19, no. 3, pp. 279-290, 2014.
- [13] J. Kulhanek, P. Tomcik, R. Trojan, M. Juranek and P. Klaus, "Experimental modeling of weld thermal cycle of the head affected zone (HAZ)," *Metalurgija* , vol. 55, pp. 733-736, 2016.
- [14] Eghlimi, M. Shamanian and K. Raeissi, "Dilution and Ferrite Number Prediction in Pulsed Current Cladding of Super-Duplex Stainless Steel Using RSM," *ASM International* , vol. 22, p. 3657–3664, 2013.
- [15] K. B. Small, D. A. Englehart and T. A. Christman, "Guide to etching speciality alloys," *Advanced Materials and Processes* , pp. 32-37, 2008.

★ ★ ★